Optimization of Aperture Transitions for Multiport Microstrip Circuits

Chinglung Chen, *Member, IEEE*, Ming-Ju Tsai, *Member, IEEE*, and Nicolaos G. Alexopoulos, *Fellow, IEEE*

***Abstract*—The introduction of printed aperture into multiport microstrip circuits as a vertical transition proves to be practical in the design as well as manufacturing process of multilayered circuits. With the mixed-potential integral equation-based moment method, it becomes possible to analyze and optimize the performance of this arbitrary shape aperture transition for multiport circuit applications. Bandwidth enhancement is obtained by changing the shape of the slot for two-port and three-port microstrip transitions. Also, the influence of slot size, orientation, and mutual coupling have been thoroughly studied in order to reach an optimal circuit performance. Using this transition, a three-port power divider with 180 degree phase difference and a directional coupler with various degree of coupling have been designed.**

I. Introduction

PRINTED SLOT has been widely utilized as a vertical transition as well as in directional coupler applications [1]–[10] of a multilayered microwave integrated circuit. In addition, coplanar waveguide and slotline are popularly used in microwave and millimeter-wave integrated circuits (MMIC's). To deal with the increase in complexity, density, and requirements in microwave circuit design, a mixed-potential integral equation (MPIE) [12]-based moment method is employed to investigate and optimize the aperture coupling effect between microstrips in multilayered media.

The application of the printed aperture as a vertical transition has been investigated intensively [2]–[6], [8]. However, since most of the previous works are either based on simplified theory or rectangular shape apertures, the investigation of the arbitrarily-shaped printed slot and its impact in bandwidth optimization is beyond their scope. A spatial-domain integral equation approach was presented recently to investigate this structure for a two-port [9]. Here, we extended the MPIE's [13] and [14] to come out with concise expressions [12] which provide physical insight, easy manipulation, and numerical efficiency. In this research, the bowtie slot has been introduced successfully to enhance the transmission bandwidth coefficient by 50%. A simple change in slot orientation is used to achieve maximum coupling for two back-to-back microstrips with arbitrary crossing angle, which is realistic for practical microwave circuits. The mutual coupling between this transition and surrounding microstrip circuits is also investigated. With a reasonable spacing ($\geq \lambda_g/4$), it is observed that the mutual coupling effect can be neglected.

In addition to the study of two-ports, the same approach is extended to investigate multiport transitions such as a three-port back-to-back microstrip power divider and four-port directional coupler by using two slots. It is shown that by introducing a quarter-wavelength step discontinuity over the upper microstrip line, a good return loss can be reached for a three-port power divider. The introduction of bowtie slot also enhances the bandwidth substantially. Lastly, a directional coupler is established by properly adjusting the slot length with fixed separation distance. This research provides the versatility to design multiport microstrip circuits with the use of a printed aperture.

Manuscript received March 25, 1996. This work was supported in part by the U.S. Army under Research Grant DAAH 04-93-G-0228 and Hughes-UC Microelectronics under Contract 94-005.

C. Chen is with the Anritsu/Wiltron Company, Morgan Hill, CA 95123 USA.

M.-J. Tsai is with the Lucent Technologies, Murray Hill, NJ 07974 USA.

N. G. Alexopoulos is with the Department of Electrical Engineering, University of California, Los Angelse, Los Angeles, CA 90095 USA.

Publisher Item Identifier S 0018-9480(96)08554-7.

II. Modeling of the Problem

A. Mixed Potential Integral Equation and Moment Method

A typical structure of interest is shown in Fig. 1. The electric current $\vec{J}_1$ on the lower microstrip line, the tangential electric field $\vec{E}_2$ in the aperture, and the electric current $\vec{J}_3$ on the upper microstrip are modeled with triangular patch basis functions. An application of the equivalence principle allows the aperture to be closed and replaced with a fictitious magnetic current $\vec{M}_2 = \hat{z} \times \vec{E}_2$ below the upper ground plane and $-\vec{M}_2$ above the upper ground plane.

Galerkin's method is applied to solve the mixed-potential integral equations and acquire the electric and magnetic current distributions on the microstrips and aperture [12]. A vectorized triangular basis function [13] is found to be a good choice because its shape can be arbitrarily defined. The nth basis function is defined as

$$\vec{f}_n = \begin{cases} \dfrac{l_n}{2A_n^+}[(x - x_{1n})\hat{x} + (y - y_{1n})\hat{y}] & x, y \text{ in } T_n^+ \\ \dfrac{l_n}{2A_n^-}[(x_{4n} - x)\hat{x} + (y_{4n} - y)\hat{y}] & x, y \text{ in } T_n^- \\ 0, & \text{otherwise} \end{cases} \quad (1)$$

where $A_n^{\pm}$ is the area of the triangular face $T_n^{\pm}$ and l_n is the length of the common edge. The domain of the nth basis function is uniquely defined by the four vertices $(x_{in}, y_{in}), i = 1, 2, 3, 4$ as shown in Fig. 2. We then expand the electric and

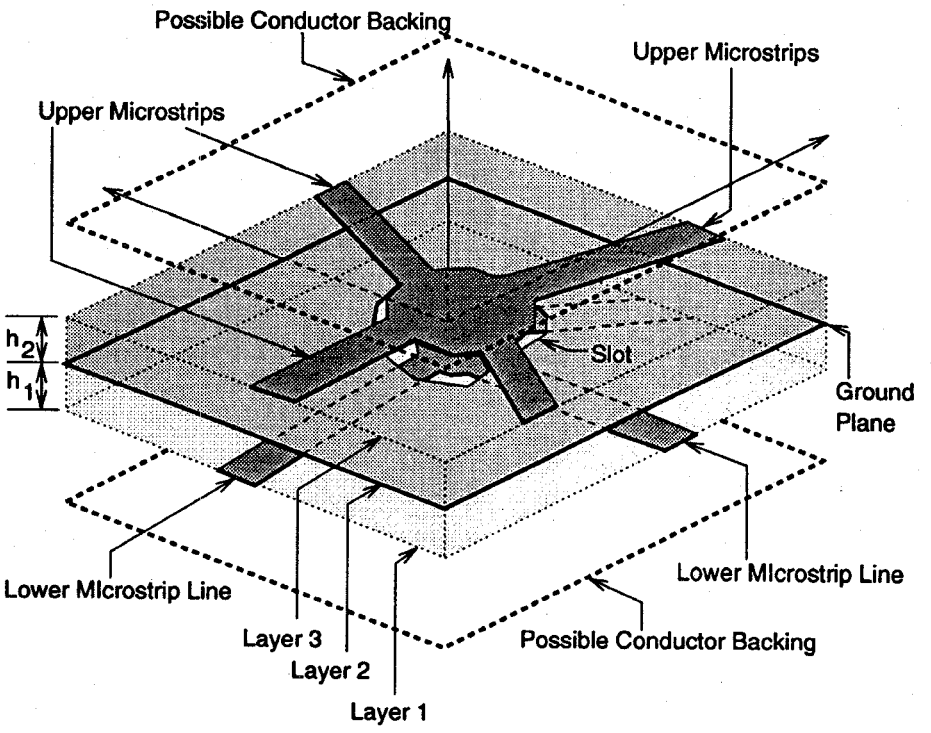

Fig. 1. Structure of a microstrip line fed aperture coupled microstrip.

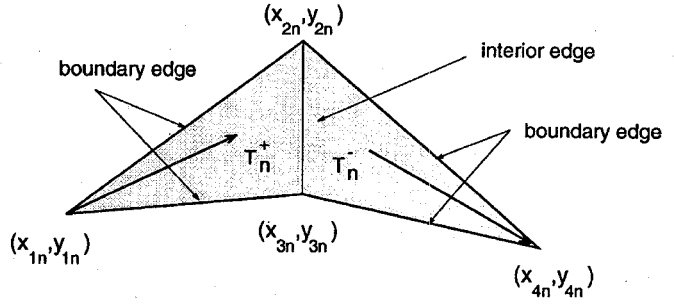

Fig. 2. Domain of the triangular basis function.

magnetic current distributions as

$$\vec{J}_1 = \sum_{n=1}^{N_1} A_n \vec{f}_{n1}, \quad \vec{M}_2 = \sum_{n=1}^{N_2} B_n \vec{f}_{n2}, \quad \vec{J}_3 = \sum_{n=1}^{N_3} C_n \vec{f}_{n3} \tag{2}$$

where $\vec{f}_{n1}$, $\vec{f}_{n2}$, and $\vec{f}_{n3}$ are arbitrarily-defined triangular basis functions located in layers 1, 2, and 3, respectively. Upon introducing these distribution functions into the mixed-potential integral equations and testing them with percentage $\vec{f}_{m1}$, $\vec{f}_{m2}$, and $\vec{f}_{m3}$, a system of linear equations will be obtained as

$$\begin{bmatrix} [\vec{E}_{\text{inc}}, \vec{f}_{m1}] \\ [\Delta\vec{H}_{\text{inc}}, \vec{f}_{m2}] \\ [0] \end{bmatrix} = \begin{bmatrix} [Z_{11}] & [W_{12}] & [0] \\ [U_{21}] & [Y_{22}] & [U_{23}] \\ [0] & [W_{32}] & [Z_{33}] \end{bmatrix} \cdot \begin{bmatrix} [A] \\ [B] \\ [C] \end{bmatrix} \tag{3}$$

where $[Z_{ii}]$, $[W_{ij}]$, $[U_{ji}]$, and $[Y_{jj}]$ are self and mutual coupling integral submatrices between two basis functions located at

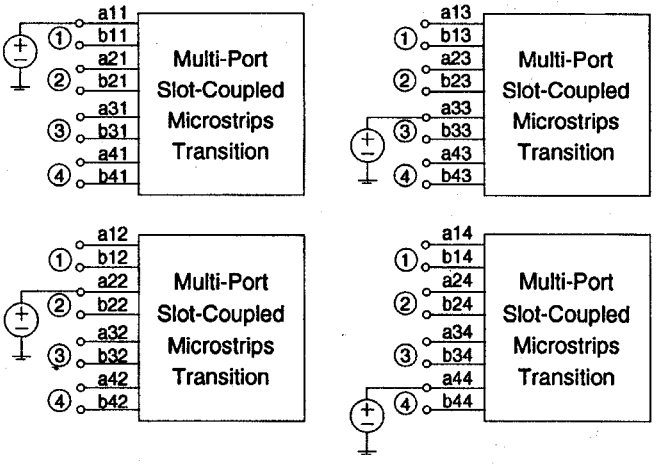

Fig. 3. De-embedding of S parameters from a four-port slot-coupled microstrip transition.

$z = -h_1, z = 0$, or $z = h_2$, respectively, $(i, j \in 1, 2, 3)$. $[A], [B]$, and $[C]$ are unknown coefficient vectors of basis functions on the microstrips and aperture, respectively. $\vec{E}_{\text{inc}}$ and $\Delta\vec{H}_{\text{inc}}$ are the incident electric and magnetic fields from the lower microstrip feed line. Once these current distributions are extracted, the scattering parameters will be calculated.

The formulas for the self-coupling submatrices have been derived in [13], [14]. The major difference of the MPIE applied here is the formulation of the mutual coupling between electric and magnetic currents [12]. This concise formulation provides not only good computational efficiency, but also gives physical insight of the coupling mechanism. We will give a brief description as follows. The mutual coupling submatrices

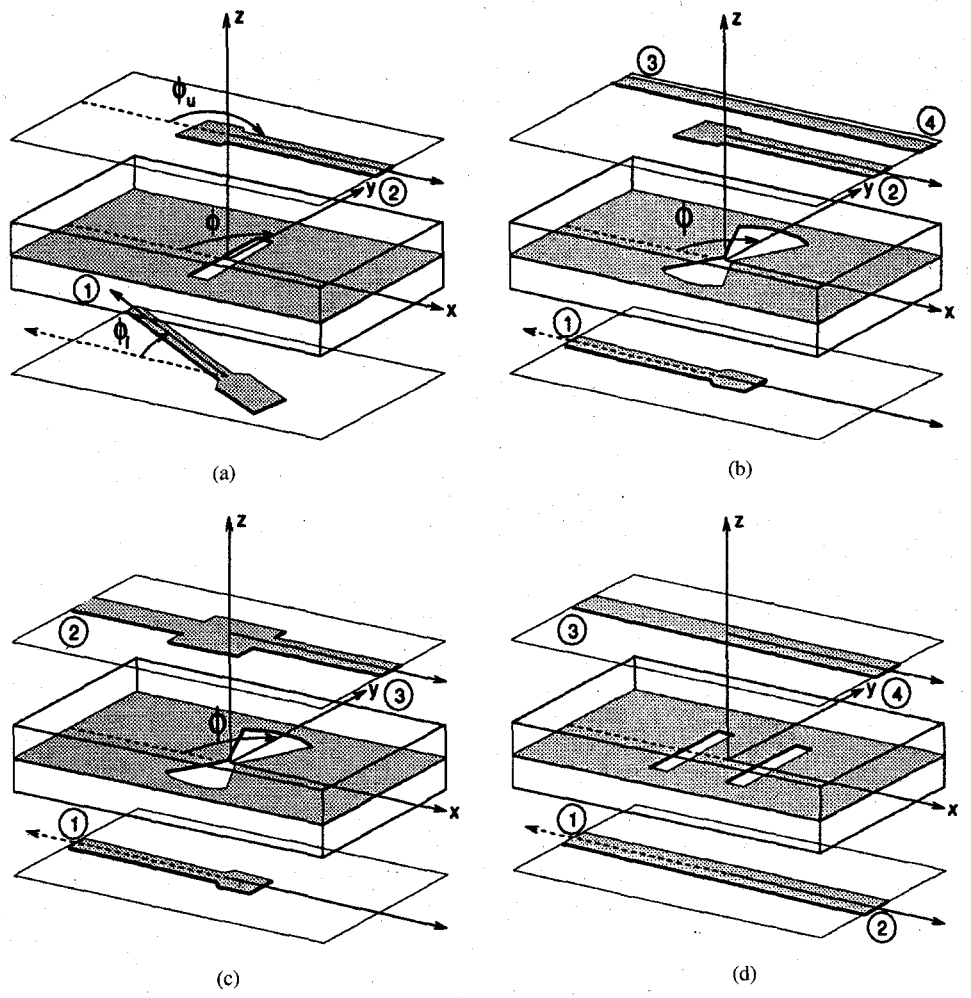

Fig. 4. Application of printed slot into multilayered microwave circuit. (a) Two-port slot-coupled microstrip transition. (b) Two-port slot-coupled microstrip transition with adjacent microstrip circuit. (c) Three-port slot-coupled power divider. (d) Four-port slot-coupled directional coupler.

$[W_{(1,3)2}]$ and $[U_{2(1,3)}]$ are formulated as

$$W^{mn}_{(1,3)2} \equiv \frac{1}{\epsilon_{(1,2)}\epsilon_0}\left\{\int_{C^{\pm}_{(1,3)m}} \vec{F}^{(L,U)}_{mn,(1,3)2,z} \cdot [\vec{f}_{m(1,3)} \times \hat{u}_m]\, dc_{(1,3)} + \int_{\Gamma^{\pm}_{(1,3)m}} \left[\frac{\partial}{\partial z}\vec{F}^{(L,U)}_{mn,(1,3)2,t} \times \vec{f}_{m(1,3)}\right] \cdot \hat{z}\, ds_{(1,3)}\right\} \tag{4}$$

$$U^{mn}_{2(1,3)} \equiv \frac{-1}{\mu_{(1,2)}\mu_0}\left\{\int_{C^{\pm}_{2m}} \vec{A}^{(L,U)}_{mn,2(1,3),z} \cdot [\vec{f}_{m2} \times \hat{u}_m]\, dc_2 + \int_{\Gamma^{\pm}_{2m}} \left[\frac{\partial}{\partial z}\vec{A}^{(L,U)}_{mn,2(1,3),t} \times \vec{f}_{m2}\right] \cdot \hat{z}\, ds_2\right\} \tag{5}$$

where $\vec{F}^{(L,U)}_{mn,(1,3)2}$ and $\vec{A}^{(L,U)}_{mn,2(1,3)}$ are the vector potential distribution functions within the testing region ($(x,y) \in \vec{f}_{m(1,2,3)}$) which is generated by the electric and magnetic current basis function $\vec{f}_{n(1,2,3)}$, respectively.

From (4), (5), the physical mechanism of the mutual coupling between electric and magnetic currents can be observed. If the medium is homogeneous, the vector potential component in vertical direction will disappear. In this case, the impedance matrix is only contributed to by a cross product between potential and testing functions (such as a stripline fed slot [12], [15], [16]). Since this vector potential component points to the same direction as the basis function, electromagnetic energy couples transversely rather than collinearly. With a multilayered substrate, the vertical-directional vector potential it will contribute to the mutual coupling.

B. De-Embedding of the Scattering Matrix for an N-Port Network

For the excitation vector, we have included an impressed electric field $\vec{E}_{\text{inc}}$ as the electric field generated by a series voltage gap source placed across the positive to negative triangles of a single basis function near the end of the microstrip feed line. In order to extract the S parameters for N-port circuitry, the following procedure is adopted to accomplish this goal. Let us take a four-port slot-coupled microstrip transition as an example. A generalized four-port needs 16 unknown S parameters ($S_{ij}; i,j = 1$ to 4) to describe

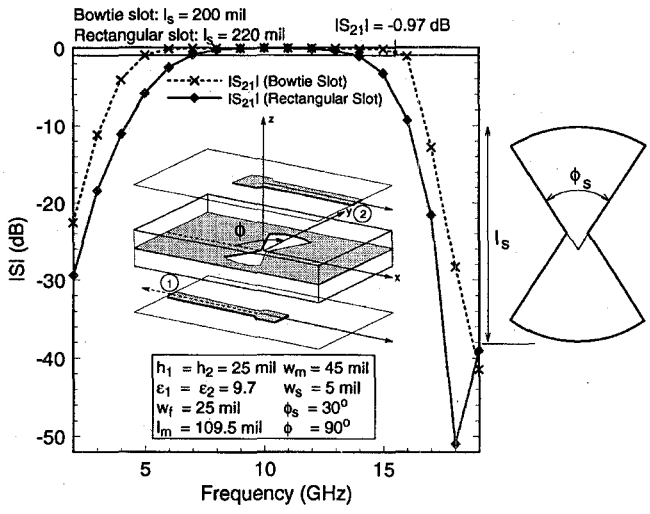

Fig. 5. Comparison of $|S_{21}|$ between two-port rectangular slot and bowtie slot-coupled microstrip transition (w_f: microstrip line width, l_m: open stub length, w_m: open stub width, l_s: slot length, w_s: slot width at $y = 0$, ϕ_s: bowtie slot arc angle).

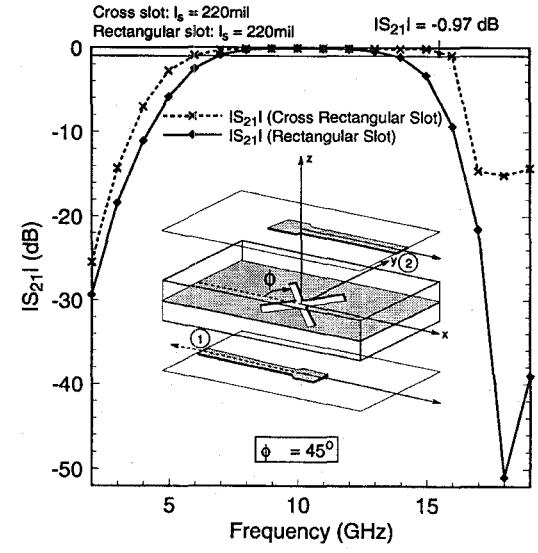

Fig. 6. Comparison of $|S_{21}|$ between two-port rectangular slot and cross rectangular slot-coupled microstrip transition (refer to Fig. 5 for details of the geometry and substrate except ϕ).

its behavior. However, every single excitation only leads to an underdetermined matrix equation as follows:

$$\begin{bmatrix} b_1 \\ b_2 \\ b_3 \\ b_4 \end{bmatrix} = \begin{bmatrix} S_{11} & S_{12} & S_{13} & S_{14} \\ S_{21} & S_{22} & S_{23} & S_{24} \\ S_{31} & S_{32} & S_{33} & S_{34} \\ S_{41} & S_{42} & S_{43} & S_{44} \end{bmatrix} \cdot \begin{bmatrix} a_1 \\ a_2 \\ a_3 \\ a_4 \end{bmatrix} \tag{6}$$

where a_i and b_i $(i = 1\text{–}4)$ represent the incident and reflected waves at each port, respectively. Although this equation can not be solved uniquely, we still can solve it without extra work from what has been done. First, we excite each port once to acquire a set of a_i and b_i $(i = 1\text{–}4)$ as shown in Fig. 3. Then an exact matrix equation as shown below will be obtained to produce all the scattering parameters

$$\begin{bmatrix} S_{11} & S_{12} & S_{13} & S_{14} \\ S_{21} & S_{22} & S_{23} & S_{24} \\ S_{31} & S_{32} & S_{33} & S_{34} \\ S_{41} & S_{42} & S_{43} & S_{44} \end{bmatrix} = \begin{bmatrix} a_{11} & a_{12} & a_{13} & a_{14} \\ a_{21} & a_{22} & a_{23} & a_{24} \\ a_{31} & a_{32} & a_{33} & a_{34} \\ a_{41} & a_{42} & a_{43} & a_{44} \end{bmatrix}^{-1} \cdot \begin{bmatrix} b_{11} & b_{12} & b_{13} & b_{14} \\ b_{21} & b_{22} & b_{23} & b_{24} \\ b_{31} & b_{32} & b_{33} & b_{34} \\ b_{41} & b_{42} & b_{43} & b_{44} \end{bmatrix} \tag{7}$$

where a_{ij} and b_{ij} denote the incident and reflected waves at ith port when the jth port is excited. a_{ij}'s and b_{ij}'s are extracted from the current distributions along each port (Details are shown in [16]). Each time we excite this slot-coupled microstrip transition at a different port, the left-hand side of (3) is unchanged. The inverse of the impedance-admittance matrix, which takes most of the CPU time, will only be performed once to solve (7). This means that the total effort to excite a N-port transition is almost the same as if we excite it once. As a result, the N-port S parameters can be de-embedded without much extra work.

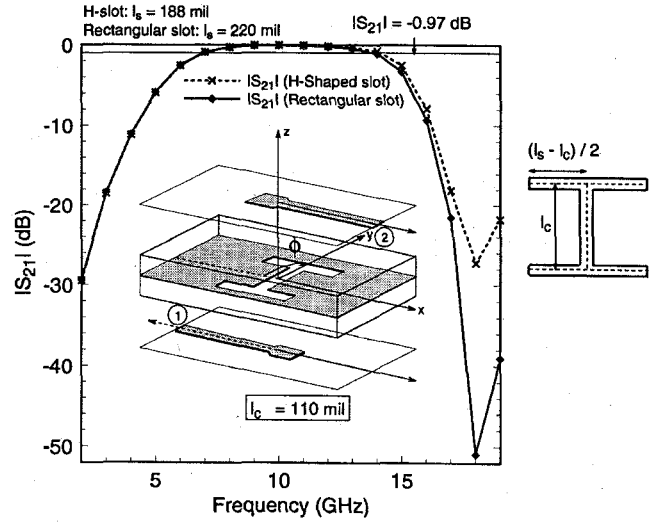

Fig. 7. Comparison of $|S_{21}|$ between two-port rectangular slot and H-shaped slot-coupled microstrip transition (refer to Fig. 5 for details of the geometry and substrate except l_s and l_c).

III. Results

A. Slot-Coupled Two-Port Microstrip Transition

In multilayered microwave integrated circuit applications, printed slots have been known to be versatile for vertical transitions. They can be implemented to couple electromagnetic energy from one side of a circuit module to another separated by a conductor. Some useful circuit applications utilizing slot-coupling transition (as shown in Fig. 4) are investigated in this work. A rectangular two-port slot-coupled microstrip transition was studied in our previous work which justifies the validity of the MPIE-based moment method. Good agreement was obtained between calculation and measurement. Having demonstrated the accuracy of this method, we use next a bowtie slot to enhance the transition bandwidth. The band-

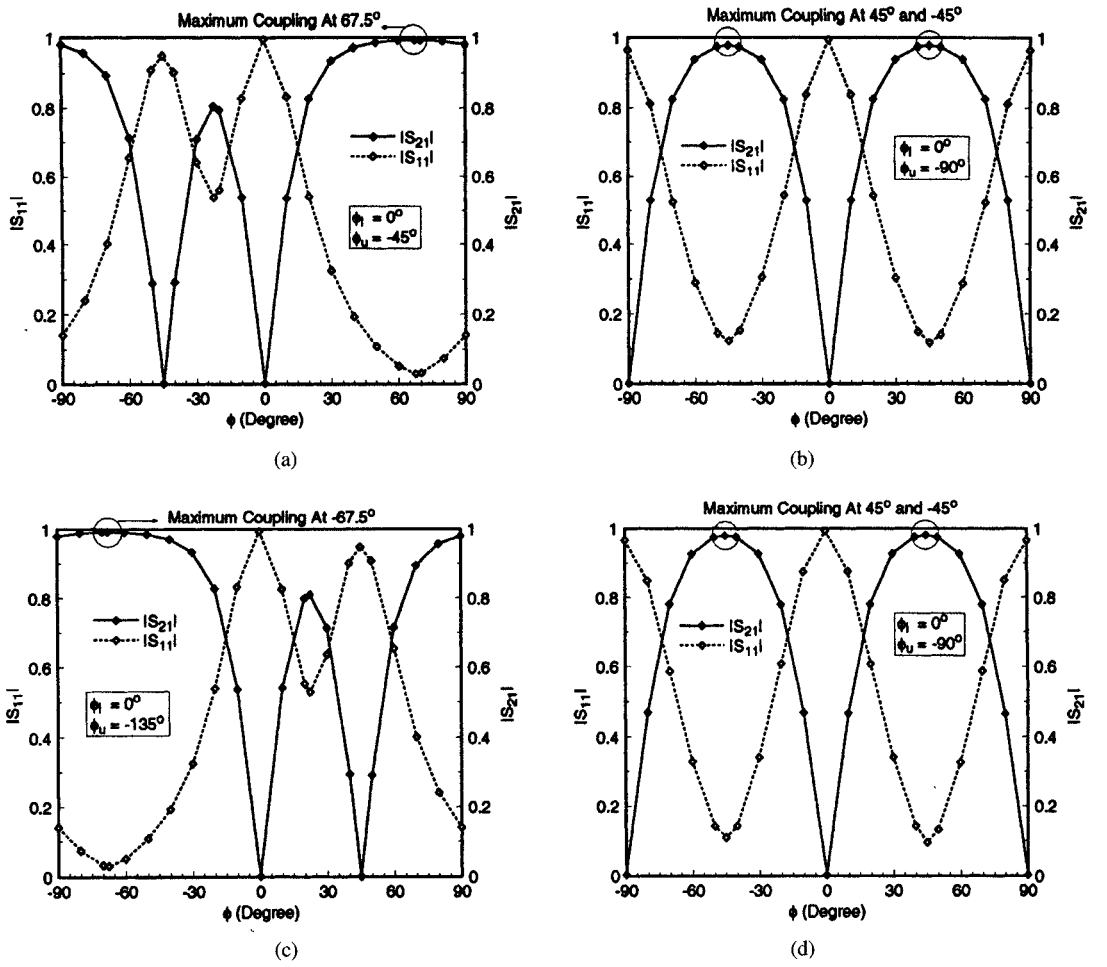

Fig. 8. S Parameters versus slot orientation angle for a two-port rectangular slot-coupled microstrip transition with crossing angles equal to 45°, 90°, 135° and a two-port bowtie slot-coupled microstrip transition with crossing angle equal to 90°, respectively, (refer to Fig. 5 for details of the geometry and substrate except ϕ, ϕ_l and ϕ_u).

width increase for the transmission coefficient can be as high as 50% as shown in Fig. 5. The larger the bowtie arc angle is, the more enhancement in bandwidth is expected. In addition, its length is reduced as compared to a rectangular-slot case. In this research, the case of a cross rectangular slot and cross bowtie slot are also studied. Similar improvement is observed as shown in Fig. 6. As a result, properly adjusting the slot shape can lead to good coupling within a wider frequency range and minimized longitudinal size, which is also critical in practical microwave circuit design.

In MIC design, the available space for the coupling slot is usually limited because of the large element density in a microwave circuit package. The previous design of slot-coupled back-to-back two-port microstrip transition can only reduce the length by about 10% compared to the case of a rectangular slot. In order to achieve a better design, a twisted H-shaped slot is introduced. Optimizing its inner length (l_c) and total length (l_s), a less than -0.5-dB S_{21} can be achieved at the center frequency (10 GHz). However, the improvement in S_{21} bandwidth is sacrificed. From Fig. 7, it is observed that this slot behaves similarly to a rectangular slot. Furthermore, it is shorter than the rectangular slot by 50% This slot generates less mutual coupling to the adjacent circuit component compared to the conventional rectangular slot. This issue will be discussed in detail later.

B. Slot-Coupled Two-Port Arbitrarily Oriented Microstrip Transition

In a realistic design, because of the limited available space, two back-to-back microstrip lines also are not always oriented collinearly. In order for effective signal transmission from one module to another, the aperture coupling between arbitrarily crossed microstrip lines has to be properly modeled and optimized. In this research, the optimal slot location is found by using a full-wave MPIE technique, and the numerical results are shown in Fig. 8. It is observed that total transmission can be reached if the orientation angle of the slot is properly chosen. From the simulated results, a simple rule can be derived to help in deciding this angle (ϕ_{opt}) as

$$\text{if } |\phi_l - \phi_u| \le 90^\circ \quad \phi_{\text{opt}} = \frac{[\phi_l + \phi_u]}{2} + 90^\circ$$

$$\text{if } |\phi_l - \phi_u| \ge 90^\circ \quad \phi_{\text{opt}} = \frac{[\phi_l + \phi_u]}{2}$$

where ϕ_l and ϕ_u are the orientation angles of lower and upper microstrip lines defined in Fig. 4(a), respectively. Once the

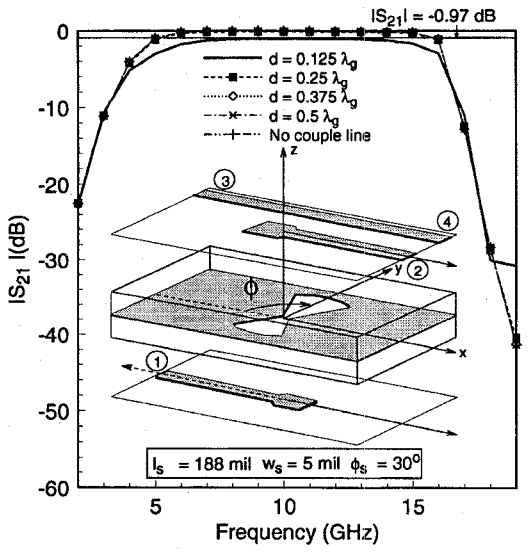

Fig. 9. $|S_{21}|$ versus Spacing (d) between upper microstrip and adjacent infinite microstrip line of a two-port bowtie slot-coupled microstrip transition (refer to Fig. 5 for details of the geometry and substrate except l_s).

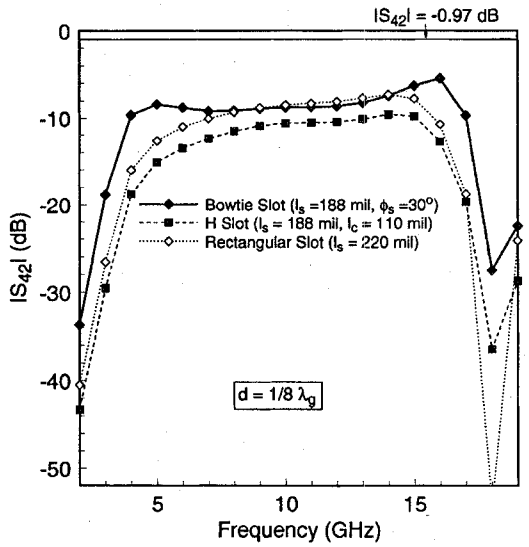

Fig. 10. $|S_{42}|$ versus spacing (d) between upper microstrip and adjacent infinite microstrip line of a two-port rectangular slot, bowtie slot, and H-shaped slot-coupled microstrip transition (refer to Fig. 5 for details of the geometry and substrate except l_s).

slot orientation angle is obtained, improvement in bandwidth and size minimization can be carried out by adjusting the slot shape as for the case of collinearly located microstrip lines.

C. Mutual Coupling Study

If the vertical coupling through slots has strong effects on the adjacent microstrip circuit, the use of apertures will not be useful in a microwave package. Since the slot is normally more than a quarter wavelength long, the effect of mutual coupling introduced by the slot is important in this design. An infinitely-long microstrip line is introduced to the upper layer of a two-port bowtie slot-coupled microstrip transition in order to study this effect. It is observed from Fig. 9 that as long as the spacing between the adjacent microstrip line and the transition

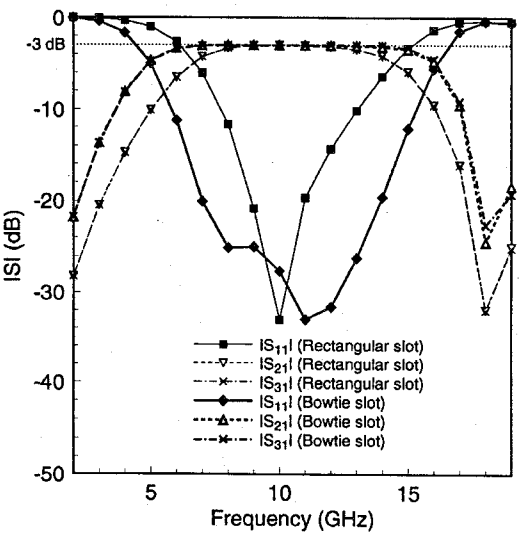

Fig. 11. Comparison of the s parameters between rectangular and bowtie slot-coupled 3-dB double-layered power divider (refer to Fig. 5 for details of the geometry and substrate except: upper microstrip step. Length: 210 mil, upper microstrip step width: 47 mil, rectangular slot length: 216 mil, rectangular slot width: 5 mil, bowtie slot length: 200 mil, bowtie slot width at $y = 0$: 5 mil).

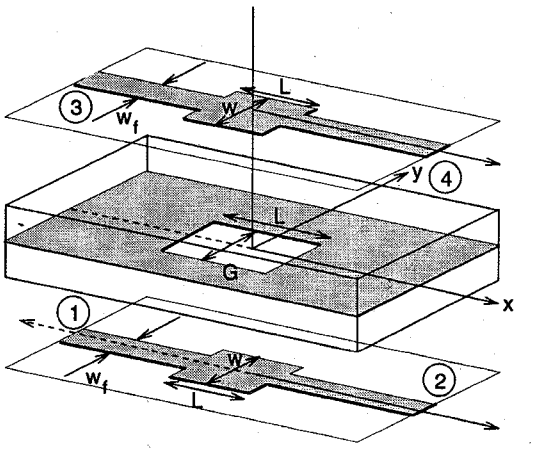

Fig. 12. Structure of a slot-coupled double-layered directional coupler.

region is equal or larger than a quarter of guided wavelength, the parasitic coupling to the adjacent microstrip line can be rejected. Different types of slots excite different amounts of mutual coupling. The mutual coupling due to rectangular slot, bowtie slot, and H-shaped slot is compared. The infinitely-long microstrip line is located at a distance of $\ell_g/8$ from the upper microstrip line, which will cause strong mutual coupling. From Fig. 10 the following observations are made.

1) At the center frequency, rectangular slot couples more energy to the adjacent microstrip line than bowtie and H-shaped slots.
2) In the upper and lower band, bowtie slot couples more energy than rectangular and H-shaped slots.

The reasons are: At the center frequency, bowtie and H-shaped slots twist the polarization direction of the out-going electromagnetic wave (the cause of the mutual coupling), from longitudinal direction ($\hat{y}$ axis) to transverse direction ($\hat{x}$ axis). Since the adjacent line aligns along the transverse direction,

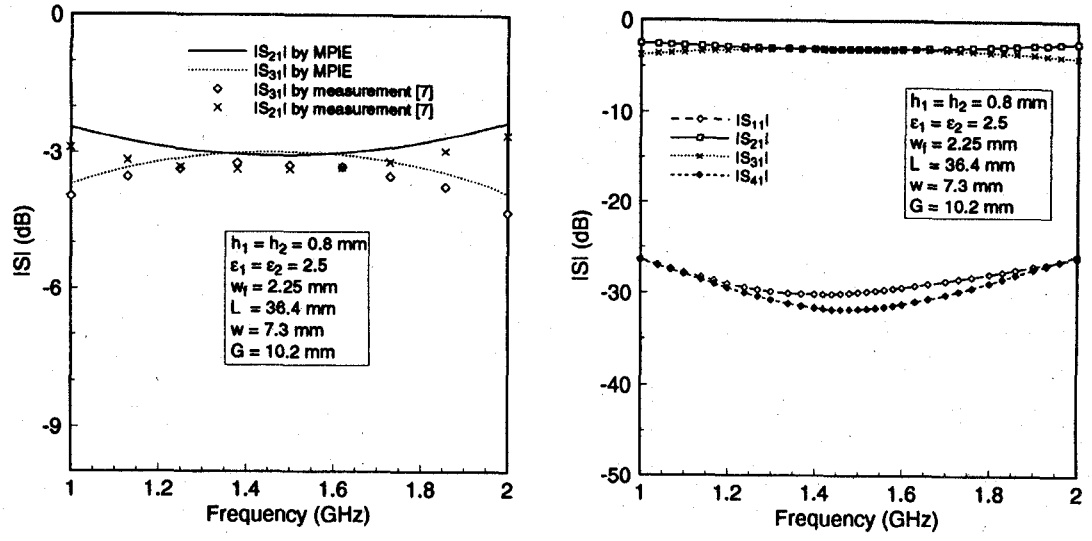

Fig. 13. S parameters of a slot-coupled double-layered 3-dB directional coupler.

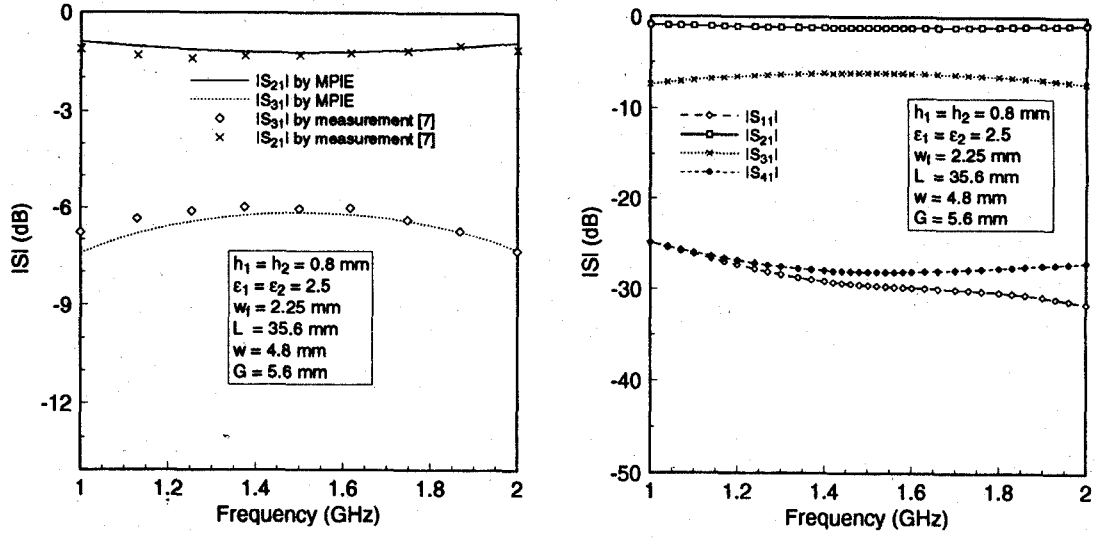

Fig. 14. S parameters of a slot-coupled double-layered 6-dB directional coupler.

the mutual coupling is reduced due to the cross product in the mutual impedance-admittance term as shown in (4) and (5). As to the higher and lower band, since the rectangular slot and H-shaped slot do not couple enough energy to the upper microstrips and slots compared to bowtie slot, the mutual coupling from the slot decreases. However, bowtie slot still offers a good coupling to the upper layer (its mutual coupling to the adjacent line is not influenced).

D. Examples of Slot-Coupled Three-Port and Four-Port Microstrip Transition

Two multiport slot-coupled microstrip circuits are investigated. The first one is a three-port power divider consisting of a terminated microstrip, an infinitely-long microstrip line with a step discontinuity, and a single slot. From Fig. 11, -3 dB equally divided signals with 180 degree phase difference appear on ports 2 and 3 of the upper microstrip line. Introducing a bowtie slot can improve the -3-dB bandwidth by approximately 60%. It is observed that if the upper microstrip line is introduced without a step discontinuity, a high return loss will appear. With a quarter-wavelength step with proper width, a good return loss performance is obtained. The same conclusion for the slot orientation angle of two arbitrarily-crossed microstrip transitions also applies here. This study suggests that this power divider can be optimized and incorporated into a microwave circuit package with no specification of location.

A four-port directional coupler using slot-coupling between back-to-back microstrip lines, as shown in Fig. 12, is also investigated. We use the MPIE technique to simulate the designs by Tanaka *et al* [7]. Two examples are shown in Figs. 13 and 14, a tight coupling 3-dB coupler and another loose coupling 6-dB directional coupler. The prediction of -3 dB and -6 dB at center frequency (1.5 GHz) are pretty accurate. The return loss and isolation are both below -25 dB. In comparison with the measured results, it is observed that the differences are within (± 0.3 dB) which can be attributed to

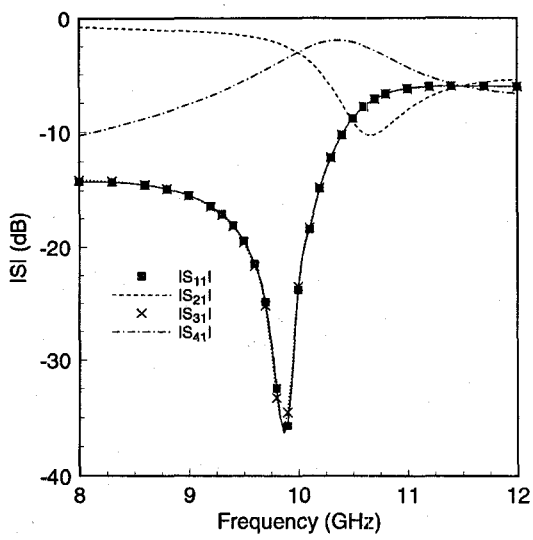

Fig. 15. S parameters of a double slot-coupled double-layered 3-dB directional coupler (refer to Fig. 5 for details of the geometry and substrate, except: slot length: 161.4 mil, interspacing between slots: 56.42 mil).

the loss from the setup of the experiments. Another directional coupler consisting of two rectangular slots separated by $\lambda_g/8$ is also designed [as shown in Fig. 4(d)]. The result are shown in Fig. 15. The idea is based on the application of quasilumped elements into quadrature coupler design by O'Caireallain *et al.* [11]. From the -3-dB transmission and coupling shown in Fig. 4, it is seen that this four-port directional coupler has good performance and will find many microwave applications.

IV. Conclusion

A concise formulation of MPIE which accounts for the mutual coupling between electric and magnetic currents in multilayered structure was applied successfully to analyze multiport slot-coupled microstrip transitions within multilayered media. A two-port slot-coupled microstrip transition was optimized to enhance the bandwidth. Mutual coupling introduced by this transition was also discussed and was found insignificant as long as the spacing between adjacent circuitries is larger than $\lambda_g/8$. With proper shape design, this mutual coupling can be further reduced while transmission bandwidth is unchanged. Lastly, a three-port power divider and four-port directional coupler using slot coupling have been investigated. The proposed structure proved to be extendible into an optimal design of a microwave antenna and circuit system containing arbitrarily-shaped microstrips, coplanar waveguides, and printed apertures.

References

[1] C. Chen and N. G. Alexopoulos, "Modeling microstrip line fed slot antennas with arbitrary shape," *Electromagn.*, vol. 15, no. 5, pp. 567–586, Sept.-Oct. 1995.

[2] H. Y. Yang and N. G. Alexopoulos, "A dynamic model for microstrip-slotline transition and related structures," *IEEE Trans. Microwave Theory Tech.*, vol. 36, no. 2, pp. 286–293, Feb. 1988.

[3] B. Schuppert, "Microstrip/slotline transitions: modeling and experimental investigation," *IEEE Trans. Microwave Theory Tech.*, vol. 36, no. 8, pp. 1272–1282, Aug. 1988.

[4] Y. M. M. Antar, A. K. Bhattacharyya, and A. Ittipiboon, "Microstripline-slotline transition analysis using the spectral domain technique *IEEE Trans. Microwave Theory Tech.*, vol. 40, no. 3, pp. 515–523. Mar. 1992.

[5] N. Herscovici and D. M. Pozar, "Full-wave analysis of aperture-coupled microstrip lines," *IEEE Trans. Microwave Theory Tech.*, vol. 39, no. 7, pp. 1108–1114, July 1991.

[6] N. L. VanderBerg and L. P. B. Katehi, "Broadband vertical interconnects using slot-coupled shielded microstrip lines, " *IEEE Trans. Microwave Theory Tech.*, vol. 40, no. 1, pp. 81–88, Jan. 1992.

[7] T. Tanaka, K. Tsunoda, and M. Aikawa, "Slot-coupled directional couplers between double-sided substrate microstrip lines and their applications," *IEEE Trans. Microwave Theory Tech.*, vol. 36, no. 12, pp. 1752–1757, Dec. 1988.

[8] A. M. Tran and T. Itoh, "Analysis of microstrip lines coupled through an arbitrarily shaped aperture in a thick common ground plane," in *IEEE MTT-S Symp. Dig,*, Atlanta, vol. 3, 1993, pp. 819–822.

[9] J. Sercu, N. Fache, F. Libbrecht, and P. Lagasse, "Mixed potential integral equation technique for hybrid microstrip-slotline multilayered circuits using a mixed rectangular-triangular mesh," *IEEE Trans. Microwave Theory Tech.*, vol. 43, no. 5, pp. 1162–1172, May 1995.

[10] R. K. Hoffmann and J. Siegl, "Microstrip-slot coupler design-part 1 and part 2," *IEEE Trans. Microwave Theory Tech.*, vol. 30, no. 8, pp. 1205–1216, Aug. 1982.

[11] S. B. S. O'Caireallain and V. F. Fusco, "Quasi-lumped element quadrature coupler design," *Microwave Opt. Technol. Lett.*, vol. 2, no. 6, pp. 216–219, June 1989.

[12] C. Chen and N. G. Alexopoulos, "Mutual coupling between microstrips through a printed aperture of arbitrary shape in multi-layered media," *IEEE Microwave Guided Wave Lett.*, vol. 6, no. 5, pp. 202–204, May, 1995.

[13] S. M. Rao, D. R. Wilton, and A. W. Glisson, "Electromagnetic scattering by surfaces of arbitrary shape," *IEEE Trans. Antennas Propagat.*, vol. 30, no. 3, pp. 409–418, May 1982.

[14] D. R. Wilton, S. M. Rao, A. W. Glisson, D. H. Schaubert, O. M. Al-Bundak, and C. M. Butler, "Potential integrals for uniform and linear source distributions on polygonal and polyhedral domains," *IEEE Trans. Antennas Propagat.*, vol.. 32, no. 3, pp. 276–281, Mar. 1984.

[15] P. S. Simon, K. McInturff, D. L. Johnson, and J. A. Troychak, "Moment method analysis of a stripline-fed finite slot using subdomain basis functions," in *1989 Antenna Applicat. Symp.*, Monticello, IL, pp. 477–505.

[16] C. Chen and N. G. Alexopoulos, "Stripline-fed arbitrarily-shaped printed aperture antennas," submitted to *IEEE Trans. Antennas Propagat.*, July 1995.

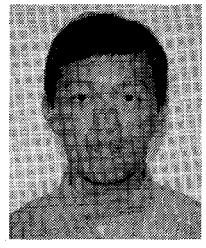

Chinglung Chen (S'92–M'96) was born in Taipei, Taiwan, R.O.C., in 1967. He received the B.S.E.E. degree from the National Taiwan University, Taipei, in 1989 and the M.S.E.E. and Ph.D. degrees from the University of California, Los Angeles (UCLA), in 1993 and 1996, respectively.

From 1989 to 1991, he served in the R.O.C. Army as a Communication Officer. Between 1992 and 1996, he was a Graduate Student Researcher in the Department of Electrical Engineering at UCLA. His work is mainly focused on numerical modeling of arbitrarily-shaped microstrips and printed slots, embedded in multilayered medium, with applications to microwave circuits and antennas. In 1996, he joined the Component Lab, MMD Division of Anritsu/Wiltron Company, Morgan Hill, CA., as a Design Engineer. His current research interests are in the area of microwave subsystem circuit design and the numerical modeling of microwave integrated circuits.

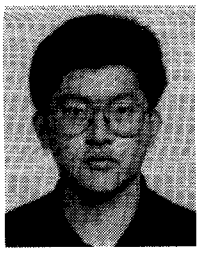

Ming-Ju Tsai (S'93–M'96) was born in Keelung, Taiwan, R.O.C., on December 17, 1966. He received the B.S.E.E. degree from the National Taiwan University, Taipei, in 1989 and the M.S.E.E. and Ph.D. degrees from the University of California, Los Angeles (UCLA), in 1993 and 1996, respectively.

He worked as a Research Assistant in the Department of Electrical Engineering at UCLA from 1992 to 1996. His work included numerical modeling of three-dimensional (3-D) multilayered microstrip structures of arbitrary shape with applications to printed circuits and antennas. In July 1996, he joined the Wireless Components and Packaging Research Department of Lucent Technologies at Murray Hill, NJ, as a Member of the Technical Staff. His research interests include the antenna modeling and design in the wireless and personal communications systems.

Dr. Tsai is also a member of editorial board of IEEE TRANSACTIONS ON ANTENNAS AND PROPAGATION.

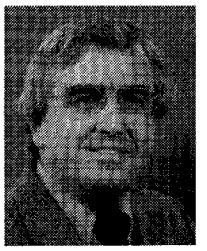

Nicolaos G. Alexopoulos (F'86) was born in Athens, Greece, on April 14, 1942. He received the B.S. degree in 1965, the M.S. degree in 1967, and the Ph.D. degree in 1968, all in electrical engineering, from the University of Michigan, Ann Arbor.

He is currently Professor of Electrical Engineering, University of California, Los Angeles. He was Associate Dean for Faculty Affairs from 1986 to 1987, and Chairman of theDepartment of Electrical Engineering from 1987 to 1992.

He was named IEEE Fellow in 1986 for "contributions to the understanding of substrate-superstrate effects on printed circuit antennas and integrated microwave circuits," and in 1985 he was co-recipient of the IEEE S.E. Schelkunoff Prize (Best Paper Award.) Since 1989, he has been Editor of *Electromagnetics*.